

Broadening of the Lyman- α line of hydrogen by low-frequency electric fields in dense plasmas

Hans R. Griem

University of Maryland, College Park, Maryland 20742

(Received 14 February 1979)

Using the quasistatic approximation as basis for the description of broadening by ion-produced fields and the impact approximation for electron-produced high-frequency fields, an analytic approximation procedure is developed and applied which allows for slow variations of the total field acting on a radiating atom. This low-frequency Stark broadening depends on the radiator velocity and is therefore correlated with the thermal Doppler broadening. The theory is extended to Lyman- α lines of hydrogenic ions.

I. INTRODUCTION

Measurements^{1, 2} of the central portions of the profiles of the Lyman- α and - β lines from optically thin plasmas revealed that the usual Stark-broadening calculations³ gave substantially less broadening than that observed experimentally. Although the deviations were much larger than experiment-theory discrepancies⁴ depending on the reduced radiator-perturbing ion mass, it was shown,^{5, 6} for the lowest density at which Lyman- α had been measured,¹ that inclusion of radiator-ion motion would greatly reduce but not eliminate the observed differences. The present author⁷ proposed a model for the inclusion of the effects from electron-produced low-frequency fields which allowed the removal of the experiment-theory discrepancy in the entire density range covered by the experiment.¹

Within the combined theoretical errors of these various attempts⁵⁻⁷ to explain the additional broadening of the Lyman- α line, one could still say that both of the two corresponding mechanisms are actually contributing to the observed broadening, i.e., both field variations associated with the relative motion of radiators and perturbing ions and field variations associated with the shielding electrons in the Debye clouds of the ions.

However, the model microfield calculation,⁶ which gives linewidths in closer agreement with measurements at all densities, seems to rule out such combined action of the two above mechanisms, since the model microfield used is produced by statically, rather than dynamically, shielded quasiparticles. A resolution of this apparent dilemma will be proposed in Sec. V. Suffice it to mention here that the smooth time variation of the actual field is in the model microfield method replaced by discrete changes in field magnitude and direction, with the frequency of these changes governed by an appropriate collision frequency in the sense that it gives the correct autocorrelation function of the field. Section II of this paper is

concerned with the effects of slowly varying electric fields, regardless of their origin, on line profiles, especially on the profile of the Stark components which in the limit of linear and static Stark effect are not affected by the field (unshifted Stark components). The magnitude of low-frequency electric field variations in dense plasmas is discussed in Sec. III, followed by Secs. IV and V devoted to combined Doppler and (low frequency) Stark effects and a comparison with experiment, respectively. Section V also contains proposed ion-dynamical corrections for Lyman- α lines from hydrogenic ions immersed in dense deuterium-tritium plasmas.

II. BROADENING BY SLOWLY VARYING ELECTRIC FIELDS

Consistent with the use of the quasistatic approximation as a point of departure, the radiating atom must be assumed to be in some electric field initially. This field $F(0)$ may be taken to be in the z direction, which is then the natural axis of quantization. Consistent with the use of the impact approximation for the broadening caused by high-frequency electron-produced fields, these fields can be assumed to vanish at $t=0$ and the atom be assumed to be at this time in one of the stationary (parabolic coordinates) eigenstates in the ion-produced but (statically) electron-shielded field $F(0)$.

Instead of Voslamber's⁵ equation (1) for the line profile of Lyman- α we start with

$$L(\omega) = \frac{1}{3\pi} \operatorname{Re} \int_0^\infty e^{-i\Delta\omega t} \left(\frac{1}{2} e^{i\omega_1 t} \langle U_{11} + U_{12} \rangle + \frac{1}{2} e^{i\omega_2 t} \langle U_{22} + U_{21} \rangle + \langle U_{33} \rangle + \langle U_{44} \rangle \right) dt. \quad (1)$$

Indices 1 and 2 designate the required linear combinations $(|210\rangle \pm |200\rangle)/\sqrt{2}$ of the two $m=0$ states, whose energies are shifted in the initial

field by $\hbar\omega_1$ and $\hbar\omega_2$, while 3 and 4 still stand for $|211\rangle$ and $|21-1\rangle$, respectively. The quantities $\langle U_{ik} \rangle$ are averages of the elements of the atomic time-evolution matrix (in the interaction representation) in the principal quantum number $n=2$ subspace, and $\Delta\omega$ is the angular frequency measured from line center. The Schrödinger equation for U , already averaged over the fast-electron time scale, is

$$\frac{dU}{dt} = \left(\frac{i}{\hbar} \vec{D} \cdot [\vec{F}(t) - \vec{F}(0)] - \mathcal{K} \right) U, \quad U(0) = 1. \quad (2)$$

The atomic-dipole operator \vec{D} and the electron-collision operator \mathcal{K} are multiplied with appropriate exponential factors, e.g.,

$$\vec{D}_{ik} = e^{i\omega_i t} \vec{D}_{ik} e^{-i\omega_k t}, \quad (3)$$

with

$$\hbar\omega_i = -\vec{D}_{ii} \cdot \vec{F}(0) = V_{ii}, \quad (4)$$

in order to account for the removal of the degeneracy with the $m=0$ states. Also, the full ion-radiator interaction $\vec{D} \cdot \vec{F}(t)$ is replaced by

$$-\vec{D} \cdot [\vec{F}(t) - \vec{F}(0)] \approx -\vec{D} \cdot \left(\frac{d}{dt} \vec{F} \right) t = \hbar\dot{\omega} t \quad (5)$$

to first order in a power-series expansion of the slowly varying part of the perturbing field. The nonvanishing components of the collision matrix are

$$\mathcal{K}_{11} = \mathcal{K}_{22} = 2w, \quad -\mathcal{K}_{12} = -\mathcal{K}_{21} = \mathcal{K}_{33} = \mathcal{K}_{44} = w, \quad (6)$$

where w is the (half) halfwidth of the electron-broadened Lorentzian profile of the central Stark components of the usual calculations.³

The coupled Schrödinger equations for one of the central (unshifted) components are

$$\frac{dU_{33}}{dt} + wU_{33} = -i\dot{\omega}_{31} t e^{i\omega_{31} t} U_{13} - i\dot{\omega}_{32} t e^{i\omega_{32} t} U_{23}, \quad (7a)$$

$$\begin{aligned} \frac{dU_{13}}{dt} + 2wU_{13} + i\dot{\omega}_{11} t U_{13} \\ = -i\dot{\omega}_{13} t e^{i\omega_{13} t} U_{33} - i\omega_{14} t e^{i\omega_{14} t} U_{43} \\ + w e^{i\omega_{12} t} U_{23}, \end{aligned} \quad (7b)$$

$$\begin{aligned} [3, 1] = & [\omega_{13}^2 - w^2 - \omega_{13}(\omega_{13}^2 - w^2)^{1/2}] \{ \gamma_1^{-2} (\gamma_1 + i\omega_{13}) w [\gamma_1^{-2} - \frac{1}{2} t^2 - \frac{1}{3} \gamma_1 t^3 + \gamma_1^{-2} e^{\gamma_1 t} (\gamma_1 t - 1)] \\ & - \gamma_2^{-2} (\gamma_2 - i\omega_{13}) (\gamma_2 - i\omega_{13} + w) [\gamma_2^{-2} - \frac{1}{2} t^2 - \frac{1}{3} \gamma_2 t^3 + \gamma_2^{-2} e^{\gamma_2 t} (\gamma_2 t - 1)] \}, \end{aligned} \quad (12)$$

and an analogous expression for $[3, 2]$. A corresponding solution can be found for the shifted components, e.g., for $U_{11} + U_{12}$. However, because the contribution of the shifted components to the central region of the line profile is small and only

$$\begin{aligned} \frac{dU_{23}}{dt} + 2wU_{23} + i\dot{\omega}_{22} t U_{23} \\ = -i\omega_{23} t e^{i\omega_{23} t} U_{33} - i\dot{\omega}_{24} t e^{i\omega_{24} t} U_{43} \\ + w e^{i\omega_{21} t} U_{13}, \end{aligned} \quad (7c)$$

$$\frac{dU_{43}}{dt} + wU_{43} = -i\dot{\omega}_{41} t e^{i\omega_{41} t} U_{13} - i\dot{\omega}_{42} t e^{i\omega_{42} t} U_{23}, \quad (7d)$$

where the frequencies in the exponents are

$$\omega_{ik} = \omega_i - \omega_k = (1/\hbar)(V_{ii} - V_{kk}),$$

$$V_{22} = -V_{11}, \quad V_{33} = V_{44} = 0.$$

The zero order solution of the coupled equations is

$$U_{33}^{(0)} = e^{-wt}, \quad U_{i3}^{(0)} = 0 \quad (i \neq 3), \quad (8)$$

which on substitution into Eqs. (7b) and (7c) and integration gives first-order solutions for U_{13} and U_{23} , e.g.,

$$\begin{aligned} U_{13}^{(1)} = & -\frac{1}{2} i \dot{\omega}_{13} e^{(i\omega_{13} - w)t} \\ & \times [\omega_{13}^2 - w^2 - \omega_{13}(\omega_{13}^2 - w^2)^{1/2}]^{-1} \\ & \times [\gamma_1^{-2} (\gamma_1 + i\omega_{13}) w (e^{\gamma_1 t} - 1 - \gamma_1 t) \\ & - \gamma_2^{-2} (\gamma_2 - i\omega_{13}) (\gamma_2 - i\omega_{13} + w) (e^{\gamma_2 t} - 1 - \gamma_2 t)], \end{aligned} \quad (9)$$

with

$$\gamma_{1,2} = \mp i(\omega_{13}^2 - w^2)^{1/2} - w. \quad (10)$$

These first-order solutions are substituted into Eq. (7a) whose integration gives a second-order solution for U_{33} ,

$$\begin{aligned} U_{33}^{(2)} = & e^{-wt} (1 - \frac{1}{2} \dot{\omega}_{31} \dot{\omega}_{13} [3, 1] \\ & - \frac{1}{2} \dot{\omega}_{32} \dot{\omega}_{23} [3, 2]), \end{aligned} \quad (11)$$

with the abbreviation

weakly dependent on frequency, low-frequency Stark broadening of these components can safely be neglected.

As shown by Demura, Lisitsa, and Sholin,⁸ one can proceed with such expressions in Eq. (1) and

arrive at complicated expressions for their averages over distributions of ion-produced fields $F(0)$ and field derivatives $\dot{F}(0)$. This is provided that one neglects correlations between perturbing ions and Debye shielding by electrons, i.e., uses distribution functions of Holtmark⁹ and Chandrasekhar and von Neumann,¹⁰ From comparisons with field distribution functions of Hooper,¹¹ which do account for correlations between perturbing charges, it is clear that the use of Holtmark, etc., functions entails large errors for the dense and low-temperature plasmas of interest here.¹ It is therefore more appropriate to simplify Eqs. (9), (11), and (12) before proceeding with the evaluation of line profiles.

For almost all values of the ion-produced field one has, e.g., $|\omega_{13}| \gg w$. This suggests to assume $w \rightarrow 0$ in all correction terms and to neglect terms involving exponential factors with ω_{13} , etc., for the calculation of the central region of the line profile. In other words, we may use here

$$U_{33} \approx U_{44} \approx e^{-wt} \left(1 - \frac{\dot{\omega}_{31}\dot{\omega}_{13} + \dot{\omega}_{32}\dot{\omega}_{23}}{\omega_{13}^2} \left(\frac{1}{2}t^2 + \omega_{13}^{-2} \right) \right) \quad (13)$$

and ignore all corrections, e.g., to $U_{11} + U_{12}$. Substitution into Eq. (1) and integration then yields for the profile of the unshifted Stark components

$$L_u(\omega) \approx \frac{2}{3\pi} \left\{ \frac{w}{w^2 + \Delta\omega^2} - \frac{1}{2} \left(\frac{\dot{F}_\perp}{wF} \right)^2 \times \left[\frac{w^5 - 3w^3\Delta\omega^2}{(w^2 + \Delta\omega^2)^3} + \left(\frac{w}{\omega_{13}} \right)^2 \frac{w}{w^2 + \Delta\omega^2} \right] \right\}, \quad (14)$$

if one also uses the relations between the various matrix elements, namely, $|z_{11}| = 2|x_{13}| = 2|y_{13}|$, and introduces $\dot{F}_\perp^2 = \dot{F}_x^2 + \dot{F}_y^2$ for the square of the field derivative in the direction perpendicular to the initial field F . [Had the exponential factors been retained, we would have $U_{33}(0) = U_{44}(0) = 1$, as usual.]

Of the two correction terms, the first agrees with the results of Demura *et al.*,⁸ while the second is $\sim 20\%$ larger than their corresponding term at small $\Delta\omega$, not to mention larger deviations at larger $\Delta\omega$. These deviations are connected with the various simplifications made here, but are of little numerical importance because $(w/\omega_{13})^2$ is very small for typical values of the ion-produced field. (Estimates show that the second term is $\sim 10\%$ of the first term in the region of interest.) We will therefore neglect the second term in the following and write the correction to the Lyman- α profile due to low-frequency field fluctuations as

$$\Delta L(\omega) = \frac{1}{3\pi} \left(\frac{\dot{F}_\perp}{wF} \right)^2 \frac{w^5 - 3w^3\Delta\omega^2}{(w^2 + \Delta\omega^2)^3}. \quad (15)$$

Before proceeding with the discussion of $(\dot{F}_\perp/F)^2$, which emerges as key quantity, it is interesting to note that the form of the correlation function actually used for $\Delta L(\omega)$, namely,

$$U_{33} \approx e^{-wt} \left[1 - \frac{1}{4} \left(\frac{\dot{F}_\perp}{F} \right)^2 t^2 \right] \quad (16)$$

is also consistent with Voslamber's result.⁵ This becomes clear if we identify the angle between the field $\vec{F}(t)$ and $\vec{F}(0)$ with $\dot{F}_\perp t/F$ and expand his expression up to t^2 . Furthermore, to the same order in powers of t , the correction factor corresponds to a Gaussian profile of $1/e$ width

$$\omega_G = \left(\frac{\dot{F}_\perp}{F} \right), \quad (17)$$

to be compared with the thermal Doppler width

$$\omega_D = (2\kappa T/M)^{1/2} \omega_0/c. \quad (18)$$

Coefficients of fourth- and higher-order terms in the correction term will of course be such that the corresponding profile becomes non-Gaussian for $\Delta\omega \lesssim \omega_G$. [Judging from Voslamber's expression,⁵ the ratio of coefficients of fourth- and second-order terms is $\sim (\frac{1}{4}\omega_G)^2$, which suggests that the Gaussian profile is accurate to $\sim 10\%$ even at $\Delta\omega \approx \omega_G$.]

III. LOW-FREQUENCY FIELD FLUCTUATIONS

According to Eq. (15), the dimensionless parameter for the relative contributions of slowly varying fields to the Lyman- α profile is \dot{F}_\perp/Fw , where \dot{F}_\perp is the magnitude of the time derivative of the low-frequency field in the perpendicular direction to the initial field F , and w is the halfwidth of the electron-broadened Lorentzian profile of the unshifted components. Within the approximations made in the preceding section, we actually only need the average of $(\dot{F}_\perp/wF)^2$ over all perturber configurations or, rather, of $(\dot{F}_\perp/F)^2$, since w is independent of F for all practical purposes.

The task of determining the average of $(\dot{F}_\perp/F)^2$ for low-density high-temperature plasmas is analogous to the problem of gravitational fields produced by stars and their fluctuation moments. These fields and moments were calculated for the case of stochastically distributed stars by Chandrasekhar and von Neumann,¹⁰ who obtained

$$\left(\frac{\dot{F}_\perp}{F} \right)_{av}^2 = \frac{9}{2} (5\pi)^{1/3} \frac{\kappa T}{M_i r_0^2} \times \left[\left(1 + \frac{M_i v^2}{3\kappa T} \right) \int_0^\infty (G-I) \frac{d\beta}{\beta^{3/2}} + \frac{5}{12\pi} \frac{M_i v^2}{3\kappa T} \int_0^\infty \left(\frac{1}{3}\beta H + K \right) \frac{d\beta}{\beta^3} \right], \quad (19)$$

where M_i is the mass of the perturbing ions, v is the velocity of the radiating atom, and r_0 is the mean ion-radiator distance defined (in terms of the ion density N) by

$$\frac{4}{3} \pi N r_0^3 = 1. \quad (20)$$

The functions G , I , and K can all be expressed in terms of the Holtmark function^{9, 10} $H(\beta)$, which for noninteracting point charges represents the distribution of reduced electric field magnitudes, i.e., of

$$\beta = F/F_0 = \left(\frac{15}{4}\right)^{2/3} F/2\pi eN^{2/3} \approx r_0^2 F/e. \quad (21)$$

The integrals in Eq. (19) can be performed analytically using the integral representations and differential equations for the various functions,¹⁰ and changing the order of integration. The result is, for $v^2 = 3kT/M_a$,

$$\begin{aligned} \left(\frac{\dot{F}_\perp}{F}\right)_{\text{av}}^2 &= \frac{3}{2} (5\pi)^{1/3} \Gamma\left(\frac{1}{3}\right) \frac{\kappa T}{M_r r_0^2} \\ &+ \frac{5}{72} \left(\frac{25}{\pi}\right)^{2/3} \Gamma\left(\frac{1}{3}\right) \frac{\kappa T}{M_a r_0^2} \\ &\approx 10.06 \frac{\kappa T}{M_r r_0^2} + 0.74 \frac{\kappa T}{M_a r_0^2} \approx 10 \frac{\kappa T}{M_r r_0^2}, \end{aligned} \quad (22)$$

and the second term, which comes entirely from the thermal motions of the radiating atoms (of mass M_a) is seen to be negligibly small. The remainder, involving the reduced mass $M_r = (M_i^{-1} + M_a^{-1})^{-1}$, conforms with the fluctuation moments used by Demura *et al.*,⁸ but it is in excess of Voslamber's estimate⁵ by a factor ~ 2 , if one uses again $\vartheta \approx (\dot{F}_\perp/F)t$ for the angle between field directions at times t and $t=0$.

In the plasmas of interest, ions and electrons do interact rather strongly. This is indicated by the typical magnitude (~ 0.6) of the dimensionless parameter r_0/ρ_D , ρ_D being the Debye length

$$\rho_D = (\kappa T/4\pi Ne^2)^{1/2}. \quad (23)$$

These interactions, first of all, lead to substantial modifications of the distribution of quasistatic fields, in the sense that relatively small fields become more probable. Since such small fields are produced by a number of perturbers acting simultaneously, the quantity $(F_\perp/F)^2$ might be expected to decrease as a result of such interactions. This seems to contradict a calculation by Hey,¹² who generalized Chandrasekhar and von Neumann's theory to the case of fields from Debye-shielded point charges. Quantitative estimates using Hey's generalization of the G , I , K , and H functions, however, are not possible because

of the large values of the expansion parameter, r_0/ρ_D , and the appearance of a minimum permissible value of β ($\sim r_0^2/\rho_D^2$) in Hey's work.

So far, we have only discussed low-frequency field variations due to ion-radiator motion. As emphasized before,⁷ we must also consider low-frequency fields produced by electrons that make up the Debye-shielding clouds of the ions. (Remember that high-frequency electron-produced fields contribute in the impact approximation to the Lorentzian width w .) These contributions to \dot{F}_\perp^2 could be estimated from standard plasma theory, provided one assumes them to be independent of the ion-produced field F . Nevertheless, in view of the difficulties with this approach for the plasma wave numbers ($k \approx 1/r_0$) and frequencies ($\omega \approx \omega_{pi}$) of interest, and because of the problems connected with the separation of corresponding ion-produced fields from the quasistatic field, we instead employ the following model:

The total field acting on a given radiator is composed of its initial value, an ion-produced slowly varying part, and a low-frequency wave-produced part, i.e.,

$$\vec{F}(t) = \vec{F}_i(0) + [\vec{F}_i(t) - \vec{F}_i(0)] + \sum \vec{F}_\omega e^{i\omega t}. \quad (24)$$

At $t=0$ and assuming random phases for the \vec{F}_ω , only the first term contributes. It cannot, however, be identified with the quasistatic field of Hooper,¹¹ which contains also some low-frequency wave contributions, but rather with the ion field of Holtmark.⁹ For the quantity of interest our model gives

$$\left(\frac{\dot{F}_\perp}{F}\right)_{\text{av}}^2 = \left(\frac{\dot{F}_\perp^2}{F_i^2 + F_w^2}\right)_{\text{av}} + \frac{2}{3} \frac{\sum \omega^2 F_\omega^2}{F_i^2 + F_w^2} \text{average}, \quad (25)$$

if we assume ion- and wave-produced parts to be independent and introduce

$$F_w^2 = \sum F_\omega^2. \quad (26)$$

The remaining average is over the magnitudes of the various ion-produced fields $F_i(0)$.

A fluid model for the plasma (see Appendix) results in

$$\begin{aligned} F_w^2 &= \frac{24}{\pi^{1/3} 5^{2/3}} F_0^2 \frac{r_0}{\rho_D} x_m \\ &\times \left[1 - \frac{2^{3/2}}{x_m} \tan^{-1} \frac{x_m}{\sqrt{2}} + \frac{1}{x_m} \tan^{-1} x_m \right]. \end{aligned} \quad (27a)$$

Here $x_m = k_m \rho_D$ corresponds to the maximum wave number k_m , beyond which a continuum description of the plasma is invalid. In analogy to the

Debye theory of specific heats of solids, we determine k_m by equating the number of wave modes times two for the two degrees of freedom per mode with the degrees of freedom of the ions in velocity space, i.e., we choose $k_m = 3(\frac{1}{4}\pi)^{1/3} r_0^{-1}$, corresponding to

$$F_w^2 = \frac{72}{20^{1/3} 5} F_0^2 \left[1 - \frac{2^{3/2}}{x_m} \tan^{-1} \frac{x_m}{\sqrt{2}} + \frac{1}{x_m} \tan^{-1} x_m \right] \equiv \beta_w^2 F_0^2. \quad (27b)$$

The same model also yields

$$\begin{aligned} \frac{2}{3} \Sigma (\omega - \vec{k} \cdot \vec{v})^2 F_\omega^2 = & \frac{36\pi^{2/3}}{5^{4/3}} \frac{\kappa T}{M_i r_0^2} F_0^2 \left\{ \left[1 - \frac{6}{x_m^2} + \frac{15}{2x_m^3} \tan^{-1} x_m - \frac{3}{2x_m^2(x_m^2+1)} \right] \right. \\ & \left. + \frac{1}{3} \frac{M_i v^2}{\kappa T} \left[1 - \frac{9}{x_m^2} + \frac{2^{5/2}}{x_m^3} \tan^{-1} \frac{x_m}{\sqrt{2}} - \frac{3}{x_m^3} \tan^{-1} x_m \right] \right\}. \end{aligned} \quad (28b)$$

With Eqs. (25), (27b), and (28b) the proposed replacement for Eq. (19) becomes

$$\begin{aligned} \left(\frac{\dot{F}_\perp}{F} \right)_{av}^2 = & \frac{9}{2} (5\pi)^{1/3} \frac{\kappa T'}{M_i r_0^2} \left(1 + \frac{M_i v^2}{3\kappa T} \right) \\ & \times \int_0^\infty \frac{\beta^{1/2}(G-I)}{\beta^2 + \beta_w^2} d\beta \\ & + \frac{36\pi^{2/3}}{5^{4/3}} \frac{\kappa T}{M_i r_0^2} \left(f_i + \frac{1}{3} f_a \frac{M_i v^2}{\kappa T} \right) \\ & \times \int_0^\infty \frac{H}{\beta^2 + \beta_w^2} d\beta, \end{aligned} \quad (29a)$$

where f_i and f_a are the factors in square brackets in Eq. (28b). Again using the integral representations for G , I , and H and noting that the integrands are even functions of β , the two integrals over β can be done first, by contour integration, and we finally obtain

$$\begin{aligned} \left(\frac{\dot{F}_\perp}{F} \right)_{av}^2 = & \frac{9}{4} 5^{1/3} \pi^{5/6} \left(\frac{8 + 4\beta_w + 2\beta_w^2}{3\beta_w^2(1+\beta_w)^{1/2}} - \frac{8}{3\beta_w^2} \right) \\ & \times \left[\frac{\kappa T}{M_i r_0^2} + \frac{1}{3} \left(\frac{v}{r_0} \right)^2 \right] + \frac{36\pi^{2/3}}{5^{4/3}} (1+\beta_w)^{-2} \\ & \times \left[f_i \frac{\kappa T}{M_i r_0^2} + \frac{1}{3} f_a \left(\frac{v}{r_0} \right)^2 \right]. \end{aligned} \quad (29b)$$

For the Lyman- α experiment,¹ the terms involving the ion mass (argon) are negligible for practically all radiator velocities v . The radiator motion

$$\begin{aligned} \frac{2}{3} \Sigma \omega^2 F_\omega^2 = & \frac{16}{15(5\pi)^{1/3}} \frac{\kappa T}{M_i r_0^2} F_0^2 \left(\frac{r_0}{\rho_D} x_m \right)^3 \\ & \times \left(1 - \frac{6}{x_m^2} + \frac{15}{2x_m^3} \tan^{-1} x_m - \frac{3}{2x_m^2(x_m^2+1)} \right), \end{aligned} \quad (28a)$$

if we neglect radiator motion. To include the latter effect, which corresponds to Doppler-shifted field fluctuations, ω^2 must be replaced by $(\omega - \vec{k} \cdot \vec{v})^2$, where \vec{v} is the velocity vector of a given radiator. On the average over \vec{k} directions this becomes $\omega^2 + \frac{1}{3} k^2 v^2$. (The term $2\omega \vec{k} \cdot \vec{v}$ does not contribute for isotropic plasmas.) Using again the fluid model (see Appendix), the required generalization is therefore

terms and their sum are shown in Fig. 1, relative to the leading term of Chandrasekhar and von Neumann,¹⁰ i.e., the first term in Eq. (22) with $\kappa T/M$ replaced by $\frac{1}{3} v^2$. Almost independent of r_0/ρ_D , $(\dot{F}_\perp/F)_{av}^2$ is seen to be reduced by long-range correlations between ions and electrons, though always by less than a factor 2, and a suitable approximation for the conditions of the experiment¹ ($\beta_w^2 \approx 2.72$, $f_a \approx 0.76$) is

$$\left(\frac{\dot{F}_\perp}{F} \right)_{av}^2 \approx \frac{1}{3} (5v/2r_0)^2. \quad (30)$$

This is a factor ~ 1.6 below the leading term of Chandrasekhar and von Neumann, which was used by Demura *et al.*,⁸ but still slightly larger ($\sim 20\%$) than Voslamber's estimate.⁵ These authors moreover, replaced v by a mean value, i.e., they did not treat the correlation between Stark and Doppler broadening. This correlation is the subject of Sec. IV.

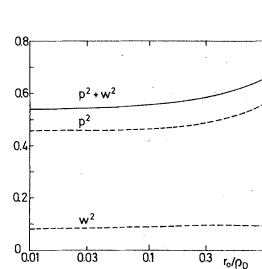


FIG. 1. Perpendicular low-frequency field fluctuations $(\dot{F}_\perp/F)^2$, relative to the fluctuations from stochastically distributed ions, as function of r_0/ρ_D (ratio of mean ion-ion separation and Debye radius). The contributions from ion-produced (P^2) and low-frequency wave-produced fields (W^2) are also shown.

IV. STARK AND DOPPLER BROADENING

We infer from Eqs. (17) and (30) that radiation emitted by atoms of given velocity has, due to low-frequency electric field fluctuations, a near Gaussian line shape of $1/e$ width

$$\omega_G \approx (5/2\sqrt{3})v/r_0 = \omega'_G v/v_a, \quad v_a = (\kappa T/M_a)^{1/2}, \quad (31)$$

or, if we allow for the Doppler shift $\omega_0(v/c)\cos\vartheta$ of the radiation, where ϑ is the angle between velocity vector and line of sight,

$$\begin{aligned} L_G(\omega) &= (2\sqrt{\pi}\omega_D)^{-1} \int_0^\infty \frac{v dv}{v_a^2} \exp\left(-\frac{v^2}{2v_a^2}\right) \left[\operatorname{erf}\left(\frac{\Delta\omega v_a}{\omega'_G v} + \frac{\omega_D}{\sqrt{2}\omega'_G}\right) - \operatorname{erf}\left(\frac{\Delta\omega v_a}{\omega'_G v} - \frac{\omega_D}{\sqrt{2}\omega'_G}\right) \right] \\ &= (2\sqrt{\pi}\omega_D)^{-1} \int_0^\infty e^{-x} dx \left[\operatorname{erf}\left(\frac{\Delta\omega}{(2x)^{1/2}\omega'_G} + \frac{\omega_D}{\sqrt{2}\omega'_G}\right) - \operatorname{erf}\left(\frac{\Delta\omega}{(2x)^{1/2}\omega'_G} - \frac{\omega_D}{\sqrt{2}\omega'_G}\right) \right], \end{aligned} \quad (33)$$

if we use Eq. (18) for the Doppler width ω_D and introduce $\Delta\omega = |\omega - \omega_0|$. Assuming the constant terms in the arguments of the error function to be small, i.e.,

$$\frac{\omega_D}{\sqrt{2}\omega'_G} \approx \frac{2\sqrt{3}}{5} \frac{\omega_0 r_0}{c} = \frac{4\sqrt{3}\pi}{5} \frac{r_0}{\lambda_0} \ll 1, \quad (34)$$

we may replace the error functions by the first two terms of their power series and obtain¹³

$$\begin{aligned} L_G(\omega) &\approx \frac{\sqrt{2}}{\pi\omega'_G} \int_0^\infty \exp\left[-x - \frac{1}{2x} \left(\frac{\Delta\omega}{\omega'_G}\right)^2\right] dx \\ &= \frac{2}{\pi} \frac{\Delta\omega}{(\omega'_G)^2} K_1\left(\sqrt{2} \frac{\Delta\omega}{\omega'_G}\right), \end{aligned} \quad (35)$$

where K_1 is a modified Bessel function. This analytic approximation, which could have been obtained more directly by neglecting the Doppler shift in Eq. (32) and then averaging over radiator velocities, remains rather accurate even for values of $\omega_D/\sqrt{2}\omega'_G$ approaching 1, as can be seen from Fig. 2, where results of numerical integrations of Eq. (33) are compared with Eq. (35). Such accuracy might have been expected, because even at $\Delta\omega = 0$, where the expansion used to obtain Eq. (35) is entirely invalid, we obtain

$$\begin{aligned} L_G(0) &= \frac{1}{\sqrt{\pi}\omega_D} \operatorname{erf}\left(\frac{\omega_D}{\sqrt{2}\omega'_G}\right) \\ &= \frac{\sqrt{2}}{\pi\omega'_G} \left[1 - \frac{1}{6} \left(\frac{\omega_D}{\omega'_G}\right)^2 + \frac{1}{40} \left(\frac{\omega_D}{\omega'_G}\right)^4 \right. \\ &\quad \left. - \frac{1}{336} \left(\frac{\omega_D}{\omega'_G}\right)^6 + \dots \right], \end{aligned} \quad (36)$$

to be compared with $\sqrt{2}/\pi\omega'_G$ from the analytic approximation. (In the experiment,¹ $\omega_D/\sqrt{2}\omega'_G$ remains below 0.5.) However, deviations from a

$$\begin{aligned} L_v(\omega) &= (2\sqrt{\pi}\omega_G)^{-1} \\ &\int_0^\pi \exp\left(-\left[\frac{\omega - \omega_0 - \omega_0(v/c)\cos\vartheta}{\omega'_G}\right]^2\right) d\cos\vartheta \\ &= \frac{c}{4\omega_0 v} \left[\operatorname{erf}\left(\frac{\omega - \omega_0 + \omega_0 v/c}{\omega'_G}\right) \right. \\ &\quad \left. - \operatorname{erf}\left(\frac{\omega - \omega_0 - \omega_0 v/c}{\omega'_G}\right) \right]. \end{aligned} \quad (32)$$

Averaged over a Maxwell distribution of velocities, this leads to

Gaussian with $1/e$ width $(\omega_D^2 + 3\omega_G'^2)^{1/2}$, i.e., from the combined Doppler and (low-frequency) Stark profiles analogous to previous calculations,⁵⁻⁸ are rather large in the parameter range of interest (see also Fig. 2). Of these deviations, those near the line center are most important. Here use of a single Gaussian profile clearly leads to an overestimate of the broadening by low-frequency fields, as did the use⁸ of Chandrasekhar and von Neumann's result¹⁰ for field fluctuations.

At large distances from line center, we have

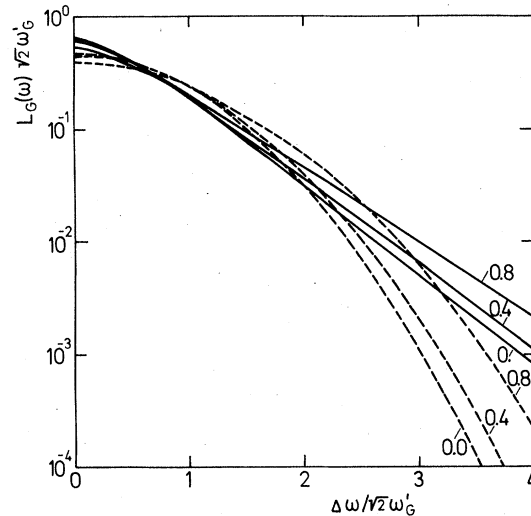


FIG. 2. Combined low-frequency Stark and Doppler profiles (solid curves) and profiles in which the velocity dependence of the effective-field fluctuations is neglected (dashed curves). The parameter on the curves is $\omega_D/\sqrt{2}\omega'_G$, the ratio of Doppler and low-frequency Stark width (times $\sqrt{2}$ and taken at the mean velocity of radiating atoms) according to Eq. (34).

from the asymptotic relations for $K_1(z)$,

$$L_C(\Delta\omega) \sim \frac{2^{1/4}}{\sqrt{\pi}} \frac{\Delta\omega^{1/2}}{(\omega'_G)^{3/2}} \exp\left(-\sqrt{2} \frac{\Delta\omega}{\omega'_G}\right) \times \left[1 + \frac{3}{2^4} \frac{\sqrt{2} \omega'_G}{\Delta\omega} - \frac{15}{2^8} \left(\frac{\sqrt{2} \omega'_G}{\Delta\omega}\right)^2 + \dots\right]. \quad (37)$$

This differs substantially from a Gaussian, but this deviation as such would not be serious, because for $\Delta\omega > \sqrt{2} \omega'_G$ electron impact broadening tends to dominate. To account for this process, we convolve $L_C(\Delta\omega)$ with a Lorentzian profile, $L_L = \pi^{-1} w(w^2 + \Delta\omega^2)^{-1}$. This leads with Eq. (35) to

$$L_C(\omega) = \left(\frac{2}{\pi\omega'_G}\right)^2 \operatorname{Re}(w + i\Delta\omega) \int_0^\infty \frac{\omega' K_1(\sqrt{2} \omega' / \omega'_G)}{(w + i\Delta\omega)^2 + \omega'^2} d\omega' \\ = \operatorname{Re} \frac{w + i\Delta\omega}{\omega'_G{}^2} \left[|H|_1 \left(\sqrt{2} \frac{w + i\Delta\omega}{\omega'_G} \right) - Y_1 \left(\sqrt{2} \frac{w + i\Delta\omega}{\omega'_G} \right) - \frac{2}{\pi} \right], \quad (38)$$

using an integral¹⁴ of this form and symmetry or recurrence relations for Bessel (Y_n) and Struve ($|H|_n$) functions.

Examples of such profiles, which account for electron impact and low-frequency Stark broadening of the unshifted components of Lyman- α are shown on Fig. 3. These profiles were calculated from Eq. (38), using the integral representation¹⁵

$$|H|_1(z) - Y_1(z) = \frac{2z}{\pi} \int_0^\infty (1+t^2)^{1/2} e^{-zt} dt. \quad (39)$$

or Gauss-Laguerre quadrature of Eq. (38). For large separations from line center, an asymptotic formula¹⁵ can be employed

$$L_C(\omega) \sim \frac{2}{\pi\omega'_G} \operatorname{Re} \left[\frac{1}{2} \left(\frac{\omega'_G}{w + i\Delta\omega} \right) - \frac{1^{23}}{2^2} \left(\frac{\omega'_G}{w + i\Delta\omega} \right)^3 + \frac{1^{23} 25}{2^3} \left(\frac{\omega'_G}{w + i\Delta\omega} \right)^5 - \dots \right], \quad (40)$$

but no convenient approximation can be obtained for small values of $\Delta\omega$.

In principle, the profiles $L_C(\omega)$ should still be corrected for Doppler broadening. However, for the experimental conditions, i.e., $0.35 < w/\omega'_G < 0.55$ and $0.68 > \omega_p/\omega'_G > 0.43$, the additional broadening is not very important. From Eq. (36) and Fig. 2 one would expect the maximum intensity to be reduced by 8% or 3%, respectively, for the lowest- and highest-density conditions and neglect-

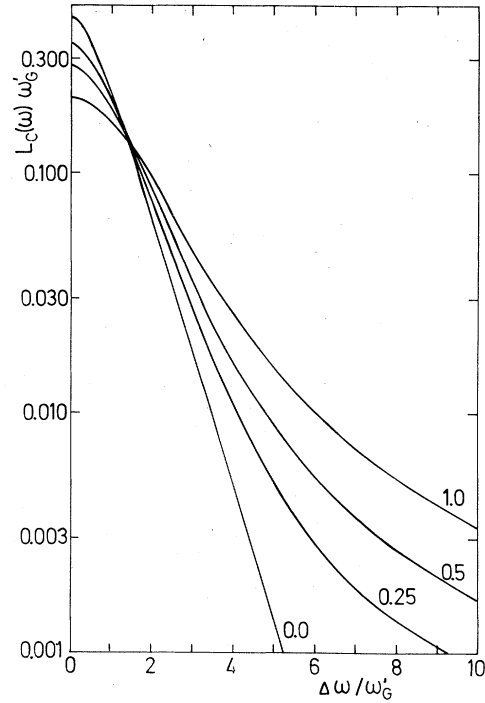


FIG. 3. Convolved low-frequency Stark and electron-impact profiles. The parameter on the curves is w/ω'_G where w is the (half) halfwidth of the Lorentz profile of ω'_G is the low-frequency Stark width at the mean velocity of radiating atoms.

ing impact broadening. According to Fig. 3, the latter effect lowers the peak intensity of the Stark profile by factors 1.43 and 1.67, respectively.

This suggests that errors from the neglect of Doppler broadening are $\sim 5\%$ at an electron density of $N = 1 \times 10^{17} \text{ cm}^{-3}$ and $\sim 2\%$ at $N = 4 \times 10^{17} \text{ cm}^{-3}$. Such errors are not only insignificant compared to those from the various approximations in the treatment of the low-frequency Stark broadening, but are also negligible compared with the large disagreement between measurements¹ and calculations^{3, 16, 17} in which Stark broadening by low-frequency fields is omitted.

V. COMPARISON WITH EXPERIMENT AND DISCUSSION

Profiles of the unshifted components according to Eqs. (38) and (39) multiplied by $\frac{2}{3}$ to account for their relative contribution to the complete profile, were added to the quasistatically and impact broadened profile¹⁶ of the shifted components and then compared with the measurements¹ at $N = 2 \times 10^{17}$ and $4 \times 10^{17} \text{ cm}^{-3}$. As can be seen in Fig. 4, the agreement is within $\sim 10\%$ over the entire range of relative intensities, to be held against a factor of ~ 1.5 disagreement near the line center and a similar factor near the half-intensity points

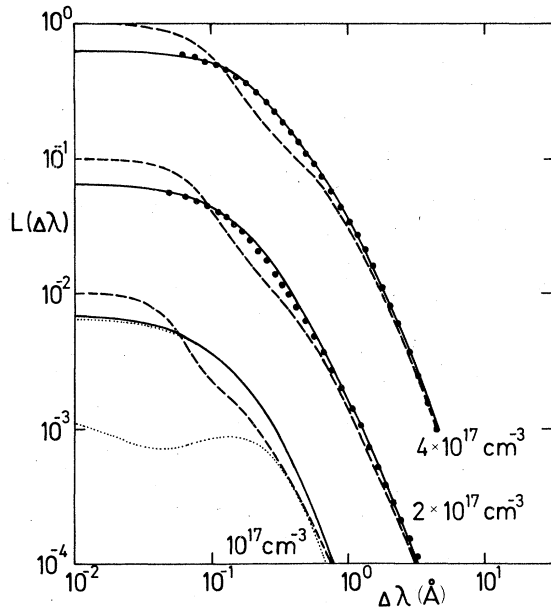


FIG. 4. Comparison of measured (heavy dots, from Ref. 1) and calculated Stark profiles (solid curves) of Lyman- α line at the indicated electron densities. Also shown are convolved Stark and Doppler profiles not accounting for low-frequency Stark effects (dashed curves, from Ref. 17) and, for the lowest density, the contribution from the shifted Stark component (lower dotted curve, from Ref. 16). The upper dotted curve for the lowest density is calculated with allowance for Doppler broadening as discussed in the text.

with calculations^{3,16,17} not allowing for low-frequency Stark effects. (Note that the shifted components, shown for $N = 10^{17} \text{ cm}^{-3}$ by the lowest curve on Fig. 4 contribute very little in the central region of the profile.) Furthermore, the agree-

TABLE I. Comparison of measured and calculated full-widths-at-half-maximum of the hydrogen Lyman- α line.

$10^{-17}N$ (cm^{-3})	$10^{-4}T$ ($^{\circ}\text{K}$)	$\Delta\lambda_{\text{ex}}^a$ (\AA)	$\Delta\lambda_{\text{th}}^b$ (\AA)	$\Delta\lambda_{\text{th}}^c$ (\AA)	$\Delta\lambda_{\text{th}}^d$ (\AA)
1	1.27	0.23	0.23(0.20)	0.20	0.19
2	1.32	0.30	0.33(0.30)	0.29	0.24
3	1.32	0.36	0.38(0.35)	0.39	0.29
4	1.40	0.42	0.44(0.42)	0.47	0.34

^a From Ref. 1.

^b Present calculations inclusive of estimated Doppler broadening (see text, values without Doppler broadening in parentheses).

^c From Ref. 7, i.e., from a model allowing for low-frequency wave-produced fields.

^d From Refs. 6 and 18, i.e., from model microfield calculations.

ment between the profiles is decidedly better than what was obtained previously⁷ on the basis of a simple physical model for the effects of low-frequency fluctuations. This model remained within the framework of the impact approximation, rather than beginning with the quasistatic approximation as the present work.

Measured and calculated halfwidths are listed in Table I. The widths calculated here tend to be larger than measured widths by $\sim 10\%$, which is, however, certainly within estimated errors of the present calculations. The only previous calculation of potentially similar accuracy, namely the model microfield calculation,⁶ yields halfwidths¹⁸ which are 20% below the measurements (see last column of Table I). One may therefore ask whether the model microfield⁶ underestimates the key quantity for corrections to the quasistatic broadening by ions, namely, $(\bar{F}_{\perp}/F)^2$.

Although this quantity does not occur directly in the model microfield calculations, it can be identified with two-thirds of the square of the jumping frequency Ω_i of the ion-produced model field. With this correspondence we find for strong fields, which dominate, e.g., in Eq. (19), for the model microfield¹⁸

$$\left(\frac{\bar{F}_{\perp}}{F}\right)^2 \approx \frac{2}{3 \cdot 0.8^2} \frac{\kappa T}{M_r r_0^2} \beta \approx \frac{\kappa T}{M_r r_0^2} \beta, \quad (41a)$$

to be compared with the asymptotic result of Chandrasekhar and von Neumann¹⁰

$$\left(\frac{\bar{F}_{\perp}}{F}\right)^2 \approx 2(\kappa T/M_r r_0^2)\beta. \quad (41b)$$

As mentioned before, our results correspond to a level of field fluctuations below those derived in Ref. 10 by a factor ~ 1.6 , so that the model microfield indeed implies values of $(\bar{F}_{\perp}/F)^2$ which are smaller than those obtained here by $\sim 20\%$, leaving as much room for wave-produced fields in this model as estimated here (see Fig. 1).

For Lyman- α lines of hydrogenic ions of nuclear charge Z , which are typically small admixtures in plasmas consisting mostly of singly charged light ions, low-frequency Stark effects per se will essentially result in a Gaussian profile with $1/e$ width given by Eqs. (17), (27b), and (29b). However, in the last equation, we now neglect the terms involving the radiator velocity v and allow for the repulsion between radiating and perturbing ions by a cutoff in the integrals over reduced fieldstrength at $\beta_m \approx (r_0/r_m)^2$ with r_m estimated by $(Z-1)e^2/r_m = \kappa T$. Assuming β_{max} to be large, the corrections are easily estimated from the asymptotic relations¹⁰ for the functions G , I , and H in Eq. (29a), and we obtain, instead of Eq. (29b),

$$\left(\frac{\dot{F}_\perp}{F}\right)_{\text{av}}^2 = \left\{ \frac{9}{4} 5^{1/3} \pi^{5/6} \left(\frac{8 + 4\beta_w + 2\beta_w^2}{3\beta_w^2(1+\beta_w)^{1/2}} - \frac{8}{3\beta_w^2} - \frac{4\sqrt{2}}{3\pi} \frac{r_m}{r_0} \right) \right. \\ \left. + \frac{36\pi^{2/3}}{5^{4/3}} f_i \left[(1+\beta_m)^{-2} - \frac{15}{28} \left(\frac{2}{\pi} \right)^{1/2} \left(\frac{r_m}{r_0} \right)^7 \right] \right\} \frac{\kappa T}{M_i r_0^2}, \quad (29c)$$

with

$$f_i = 1 - 6/x_m^2 + (15/2x_m^3)4 \tan^{-1}x_m - \frac{3}{2} x_m^{-2}(x_m^2+1)^{-1}, \\ x_m = 3(\frac{1}{4}\pi)^{1/3} \rho_D/r_0.$$

For the hydrogenlike ion of neon, which is useful as density indicator in laser fusion research as admixture to D - T plasmas, and an electron density of 10^{23} cm^{-3} at a temperature of $\kappa T = 300 \text{ eV}$, these relations give a $1/e$ width of 0.98 eV with $\beta_w = 1.874$ from Eqs. (27a) and (27b). This broadening due to low-frequency Stark effects should be compared with $\hbar\omega_c = 0.41 \text{ eV}$ from Ref. 7 and a Doppler width of 0.18 eV , while electron impact broadening¹⁹ results in a full-width-at-half-maximum of 0.31 eV . (In pure neon plasmas, low-frequency Stark effects according to the present work would come much closer to $\hbar\omega_c$. Note also that the fine-structure splitting is $\sim 0.45 \text{ eV}$ and should therefore be allowed for.)

The above example suggests that estimates for the effects of low-frequency fields proposed in Refs. 7 and 19 were indicative for Lyman- α lines of hydrogenic ions, but not quantitatively correct. Further work is needed to extend the present results to other lines of hydrogen and hydrogenic ions.

ACKNOWLEDGMENTS

The author thanks Dr. J. Seidel and Dr. D. Voslamber for their comments on the manuscript and the Humboldt Foundation and National Science Foundation for their support. Codes for $L_G(\omega)$ and $L_C(\omega)$ were written by Dr. G. Tsakiris.

APPENDIX

To estimate low-frequency field fluctuations, we begin with the two-fluid model of a plasma described by momentum equations for ions (i) and (e),

$$M_i N_i \frac{d\vec{v}_i}{dt} = eN_i \vec{E} - \kappa T \vec{\nabla} N_i, \quad (A1a)$$

$$m_e N_e \frac{d\vec{v}_e}{dt} = -eN_e \vec{E} - \kappa T \vec{\nabla} N_e, \quad (A2a)$$

the Maxwell equation for low-frequency electric fields

$$\vec{\nabla} \cdot \vec{E} = 4\pi e(N_i - N_e), \quad (A3a)$$

and the continuity equations

$$\frac{\partial N_i}{\partial t} + N_i \vec{\nabla} \cdot \vec{v}_i = 0, \quad (A4a)$$

$$\frac{\partial N_e}{\partial t} + N_e \vec{\nabla} \cdot \vec{v}_e = 0. \quad (A5a)$$

Friction between the two fluids (resistivity) can be neglected, because the collision frequency for momentum transfer between electrons and ions is much smaller than the ion plasma frequency

$$\omega_{pi} = (4\pi N e^2 / M_i)^{1/2}, \quad (A6a)$$

and we can set $m_e = 0$ because electron inertia is not important for frequencies of order ω_{pi} . The implicit assumption of equal and constant temperatures is consistent with the relatively large value of the mean free path of the particles.

We assume, as usual, that N_i and N_e are essentially equal, i.e., $N_i = N + n_i$ and $N_e = N + n_e$, and treat n_i , n_e , \vec{v}_i , \vec{v}_e , and \vec{E} as small quantities which vary as $\exp[i(kx - \omega t)]$. The linearized set of equations for the corresponding amplitudes is

$$-i\omega M_i N \vec{v}_i = eN \vec{E} - ik\kappa T \vec{n}_i, \quad (A1b)$$

$$0 = -eN \vec{E} - ik\kappa T \vec{n}_e, \quad (A2b)$$

$$ik \vec{E} = 4\pi e(\vec{n}_i - \vec{n}_e), \quad (A3b)$$

$$-i\omega \vec{n}_i + ikN \vec{v}_i = 0, \quad (A4b)$$

$$-i\omega \vec{n}_e + ikN \vec{v}_e = 0, \quad (A5b)$$

with the dispersion relation

$$(\omega/\omega_{pi})^2 = (k\rho_D)^2 [2 + (k\rho_D)^2] / [1 + (k\rho_D)^2]. \quad (A6b)$$

The following energy densities are involved in these waves: kinetic ($\frac{1}{2} M_i |\vec{v}_i|^2$), electric field ($|\vec{E}|^2/8\pi - F_\omega^2/8\pi$) and ion and electron pressures ($\frac{1}{2} \kappa T |\vec{n}_{i,e}|^2/N$). Using Eqs. (A1b)–(A5b) and Eq. (A6b) to calculate the relative contributions to the energy and assuming thermal equilibrium, i.e., a total energy κT per mode, we then obtain

$$F_\omega^2 = 4\pi(k\rho_D)^2 [1 + (k\rho_D)^2]^{-1} [2 + (k\rho_D)^2]^{-1} \kappa T, \quad (A7)$$

$$\omega^2 F_\omega^2 = 4\pi\omega_{pi}^2 (k\rho_D)^2 [1 + (k\rho_D)^2]^{-1} \kappa T. \quad (A8)$$

Multiplication with the number of modes in a unit volume, $4\pi k^2 dk / (2\pi)^3$, and integration over k finally gives Eqs. (27a) and (28a).

The waves of interest here are heavily Landau damped. This effect may be estimated by adding a Landau-damping term to the dielectric constant corresponding to the dispersion relation (A6b), i.e., by considering

$$\epsilon = \frac{1 + (k\rho_D)^2}{(k\rho_D)^2} - [2 + (k\rho_D)^2] \left(\frac{\omega}{\omega_{pi}} \right)^2 + i \left(\frac{\pi}{2} \right)^{1/2} \frac{\omega}{\omega_{pi} k\rho_D} \exp \left[-\frac{1}{2} \left(\frac{\omega}{\omega_{pi} k\rho_D} \right)^2 \right]. \quad (\text{A9})$$

Setting $|\epsilon| = 0$ and neglecting $\text{Im}\epsilon$ gives back the dispersion relation, whereas with $\text{Im}\epsilon$ and $\omega \rightarrow \omega + \Delta\omega$, we get

$$\frac{\Delta\omega}{\omega} \approx -\frac{i}{2} \left(\frac{\pi}{2} \right)^{1/2} (k\rho_D)^2 \frac{[2 + (k\rho_D)^2]^{1/2}}{[1 + (k\rho_D)^2]^{3/2}} \times \exp \left(\frac{1}{2} \frac{2 + (k\rho_D)^2}{1 + (k\rho_D)^2} \right), \quad (\text{A10})$$

i.e., damping corresponding to $\gamma = \text{Im}\Delta\omega$. Most important for us are modes with $(k\rho_D)^2 \lesssim 9(\frac{1}{4}\pi)^{2/3} (\rho_D/r_0)^2$ (see Sec. III), so that we may take the limit $(k\rho_D)^2 \rightarrow \infty$ or

$$\gamma/\omega - \frac{1}{2} \left(\frac{\pi}{2} \right)^{1/2} e^{-1/2} = 0.38. \quad (\text{A11})$$

This may not seem small, but the frequency enters only quadratically in our application so that neglecting γ^2 vs ω^2 causes errors $\lesssim 15\%$ in $\Sigma\omega^2 F_\omega^2$ and even smaller errors in ΣF_ω^2 .

¹K. Grützmacher and B. Wende, Phys. Rev. A 16, 243 (1977).

²K. Grützmacher and B. Wende, Phys. Rev. A 18, 2140 (1978).

³H. R. Griem, *Spectral Line Broadening by Plasmas* (Academic, New York, 1974).

⁴W. L. Wiese, D. E. Kelleher, and V. Helbig, Phys. Rev. A 11, 1858 (1975); see also J. L. Chotin, J. L. Lemaire, J. P. Marque, and F. Rostas, J. Phys. B 11, 371 (1978).

⁵D. Voslamber, Phys. Lett. 61A, 27 (1977).

⁶J. Seidel, Z. Naturforsch. 32a, 1207 (1977).

⁷H. R. Griem, Phys. Rev. A 17, 214 (1978); see also R. Lee, J. Phys. B 11, L167 (1978).

⁸A. V. Demura, V. S. Lisitsa, and G. V. Sholin, Sov. Phys. JETP 46, 209 (1977).

⁹J. Holtzmark, Ann. Phys. (Leipz.) 58, 577 (1919).

¹⁰S. Chandrasekhar and J. von Neumann, Astrophys. J. 95, 489 (1942); 97, 1 (1943).

¹¹C. F. Hooper, Jr., Phys. Rev. 165, 215 (1968).

¹²J. D. Hey, Trans. R. Soc. S. Afr. 42, (1), 81 (1976);

J. Quant. Spectrosc. Radiat. Transfer 16, 947 (1976).

¹³See p. 146, Eq. (29) of *Tables of Integral Transforms*, Vol. I, Bateman Manuscript Project (McGraw-Hill, New York, 1954).

¹⁴See Eq. (9) on p. 468 of G. N. Watson, *A Treatise on the Theory of Bessel Functions*, 2nd ed. (Cambridge University, Cambridge, England, 1944).

¹⁵See Eqs. 7 and 31 on pages 496 and 497, respectively, of M. Abramowitz and I. A. Stegun, *Handbook of Mathematical Functions*, Natl. Bur. St. Appl. Math. Ser. No. 55 (U.S. GPO, Washington, D.C., 1970).

¹⁶P. C. Kepple and H. R. Griem, Phys. Rev. 173, 317 (1968).

¹⁷C. R. Vidal, J. Cooper, and E. W. Smith, Astrophys. J. Suppl. Ser. 25, 37 (1973).

¹⁸J. Seidel (private communication).

¹⁹H. R. Griem, M. Blaha, and P. C. Kepple, Phys. Rev. A (to be published); see also P. C. Kepple and H. R. Griem, Naval Research Laboratory Memorandum Report 3634 (1978) (unpublished).